Available online at www.sciencedirect.com

SciVerse ScienceDirect

journal homepage: www.elsevier.com/locate/he

Short Communication

The optical absorption and hydrogen production by water splitting of (Si,Fe)-codoped anatase TiO_2 photocatalyst

Yanming Lin [a,b], Zhenyi Jiang [a,*], Chaoyuan Zhu [b], Xiaoyun Hu [c], Haiyan Zhu [a], Xiaodong Zhang [a], Jun Fan [d], Sheng Hsien Lin [b,e]

[a] Institute of Modern Physics, Northwest University, Xi'an 710069, PR China
[b] Department of Applied Chemistry, Institute of Molecular Science and Center for Interdisciplinary Molecular Science, National Chiao-Tung University, Hsinchu 30050, Taiwan
[c] Department of Physics, Northwest University, Xi'an 710069, PR China
[d] School of Chemical Engineering, Northwest University, Xi'an 710069, PR China
[e] Institute of Atomic and Molecular Sciences, Academia Sinica, Taipei 106, Taiwan

ARTICLE INFO

Article history:
Received 7 December 2012
Received in revised form
10 February 2013
Accepted 16 February 2013
Available online 16 March 2013

Keywords:
TiO_2
Codoped
Photocatalytic activity for hydrogen production
Density functional theory

ABSTRACT

The electronic and optical properties are studied using the density functional theory in (Si,Fe)-codoped anatase TiO_2. The calculated results suggest that the synergistic effects of (Si,Fe) codoping can effectively induce the redshift of optical absorption edge, which leads to higher visible-light photocatalytic activity for hydrogen production by water splitting than pure anatase TiO_2. To verify the reliability of our calculated results, nanocrystalline (Si,Fe)-codoped TiO_2 is synthesized by a sol-gel-solvothermal method, and excellent absorption performance and photocatalytic activity for hydrogen production by water splitting are observed in our experiments.

Among many candidates of semiconductor photocatalyst, titania (TiO_2) has become the most investigated one for overall water splitting for hydrogen production, due to its outstanding chemical stability, low cost, and non-toxicity [1,2]. However, the photocatalytic water splitting for hydrogen production of TiO_2 are restricted to ultraviolet (UV)-light ($\lambda < 385$ nm) due to the wide band gap of anatase TiO_2 (~3.2 eV). Therefore, reducing the band gap of anatase TiO_2 to make it photosensitive to visible-light has become one of the most important goals in photocatalytic water splitting for hydrogen production. It has been suggested that doping with different cations and anions would result in a reduced band gap for TiO_2 [3–11]. For example, Yang et al. studied systematically the nitrogen concentration influence on N-doped anatase TiO_2 [6]. The results indicate that some localized N 2*p* states are formed above the valence band in N-doped anatase TiO_2 at lower doping levels, which leads to the reduction of the photon transition energy. And the energy gap has little further

* *Corresponding author*. Tel.: +86 29 88303491; fax: +86 29 88302331.
E-mail addresses: linymnwu@gmail.com (Y. Lin), jiangzy@nwu.edu.cn (Z. Jiang).
0360-3199/$ – see front matter Copyright © 2013, Hydrogen Energy Publications, LLC. Published by Elsevier Ltd. All rights reserved.
http://dx.doi.org/10.1016/j.ijhydene.2013.02.079

narrowing compared with that at lower doping levels when the doping level rises. A few latest researches indicate that different cations and anions codoping into TiO_2 can further narrow its band gap and enhance its photocatalytic activity [12–20]. For instance, Jia et al. studied the microscopic mechanism for band gap narrowing and the origin of the enhanced visible-light photocatalytic activity in N/S-codoped anatase TiO_2 [13]. Li et al. reported that the C/H-codoping produces significant band gap narrowing, which leads to higher visible-light photocatalytic efficiency than the C-doped anatase TiO_2 [16]. The research of Su et al. suggested that the codoping of TiO_2 with N and Fe leads to the much narrowing of the band gap and greatly improves the photocatalytic activity under visible irradiation [17]. The results showed that codoping is one of the most effective approaches to extend the absorption edge to the visible-light region in anatase TiO_2. However, photocatalytic activity for hydrogen production by water splitting and optical absorption properties of (Si,Fe)-codoped TiO_2has no report on the theory and experiment. Therefore, the enhanced visible-light absorption efficiency and photocatalytic activity are expected for (Si,Fe)-codoped TiO_2.

In this letter, the electronic and optical properties of (Si,Fe)-codoped $TiO_2$are investigated using the density functional theory (DFT) to reveal the synergistic effects of (Si,Fe) codoping on the mechanism of bandgap reducing and the origin of enhanced visible-light photocatalytic activity for hydrogen production by water splitting. Nanocrystalline (Si,Fe)-codoped TiO_2 was synthesized with sol-gel-solvothermal method. It was found that the (Si,Fe)-codoped TiO_2 showed excellent photocatalytic activity for hydrogen production, which verified the reliability of our calculated results.

All the spin-polarized calculations were performed using the projector augmented wave pseudopotentials as implemented in the VASP code [21,22]. The exchange correlation function was treated by the generalized gradient approximation (GGA) with the Perdew–Wang parameterization (known as GGA-PW91) [23]. The Brillouin-zone integrations were approximated by using the special k-point sampling of the Monhkorst–Pack scheme [24]. A cutoff energy of 500 eV and a mesh size of $9 \times 9 \times 9$ were used for geometry optimization and electronic property calculations. Using the block Davidson scheme, both the atomic positions and cell parameters were optimized until the residual forces were below 0.01 eV/Å. To obtain the band gap that was consistent with the experimental result, the GGA + U method [25] was employed. The Coulombic interaction U and exchange energy J were set to be 10.0 eV and 1.0 eV, respectively. Accordingly, the calculated band gap of pure anatase TiO_2 was 2.9 eV, which was in good agreement with the experimental value [26].

The valence electron configurations considered in this study included Ti ($3d^24s^2$),O ($2s^22p^4$), Si ($3s^23p^2$), and Fe ($3d^64s^2$). All the doped systems were constructed from a relaxed ($2 \times 2 \times 1$) 48-atom anatase TiO_2 supercell and it is shown in Fig. 1(a). As the position of Fe in the TiO_2 lattice was unclear, variety of positions of Fe atoms in the lattice were considered, such as substitutional Fe at the Ti site (Fe@Ti) and O site (Fe@O). In the Si-doped TiO_2, a Ti atom is substituted by a Si atom (Si@Ti) [27]. Similar substitutions were also considered for codoped systems, as Fe locates at either Ti or O site and Si locates at Ti site, namely, Si@Ti&Fe@Ti and Si@Ti&Fe@O. To study the stabilities of the doped systems, we calculated the defect formation energy (E_f) for the doped and codoped systems according to the equations

$$E_{f(X@Y)} = E_{(X@Y)} - E_{(pure)} - (\mu X - \mu Y) \quad (1)$$

$$E_{f(Si@Y\&Fe@Y)} = E_{(Si@Y\&Fe@Y)} - E_{(pure)} - (\mu_{Si} + \mu_{Fe} - \mu_Y - \mu_Y) \quad (2)$$

where X = Si, Fe; Y = Ti, O; E represents the total energy and μ is the chemical potential. The calculated formation energies are listed in Table 1. It shows that Fe impurity is preferred to substitute Ti in lattice because of the smallest formation energy in both Fe-doped and (Si,Fe)-codoped anatase TiO_2systems.

To investigate the electronic properties of Si and/or Fe (co) doping anatase TiO_2, the total density of states (TDOS) and partial density of states (PDOS) were plotted in Fig. 2. It indicates that the valence band (VB) is dominated by O 2p states while the conduction band (CB) consists mainly of Ti 3d states for pure anatase TiO_2. In Si-doped TiO_2 (Si@Ti), the VB broadens with the mixing of O 2p and Si 3p states, and the CB bottom has a decline of about 0.15 eV, which can lead to a

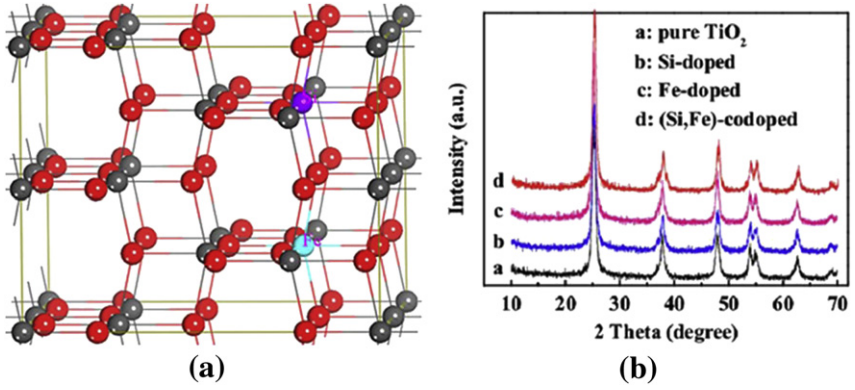

Fig. 1 – (A) 48-atom supercell model for defective anatase TiO_2 shows the location of the dopants. The atom doping sites are marked with Si and Fe. The gray spheres and red spheres represent the Ti and O atoms, respectively. The purple sphere and cyan sphere represent Si and Fe atom, respectively. (b) XRD patterns for the pure and doped TiO_2. (For interpretation of the references to colour in this figure legend, the reader is referred to the web version of this article.)

Table 1 – Defect formation energies E_f for different doped anatase TiO_2 systems.

Doped models	Doped			Codoped	
	Si@Ti	Fe@Ti	Fe@O	Si@Ti and Fe@Ti	Si@Ti and Fe@O
E_f (eV)	−8.7293	−1.5953	12.7225	−11.2535	1.7695

band gap narrowing. For Fe-doped TiO_2 (Fe@Ti), it is shown that the band gap decreases by about 0.6 eV and most Fe 3*d* states are located in the band gap compared with the pure anatase TiO_2, which may be due to stronger interactions between the Fe 3*d* and Ti 3*d* orbitals. For (Si,Fe)-codoped TiO_2 system (Si@Ti&Fe@Ti), some impurity states (Si 3*p* and Fe 3*d*) are mixed with the VB and CB edge. The top of the VB has an obvious upward shift while the CB bottom has an obvious downward shift, which results in a band gap narrowing of about 1.0 eV compared with the pure anatase TiO_2. Therefore, synergistic effect of (Si,Fe)-codoped can lead to a decrease of the photon excitation energy and redshift the optical absorption edge to the visible-light range.

According to the obtained electronic structures, we calculated the complex dielectric function $\xi = \xi_1 + i\xi_2$. The corresponding absorption spectrum was estimated by the following equation

$$I(\omega) = 2\omega\left(\frac{\left(\xi_1^2(\omega)+\xi_2^2(\omega)\right)^{1/2}-\xi_1(\omega)}{2}\right)^{1/2} \quad (3)$$

where I is the optical absorption coefficient, ω is the angular frequency ($E = \hbar\omega$).

The absorption spectra of the pure and doped anatase TiO_2 systems are calculated and shown in Fig. 3. It is found that pure anatase TiO_2 can only respond to the UV-light and shows no absorption activity in the visible-light region. For Si-doped system, it is clear that the narrowed band gap can result in the reduction of the photon transition energy from the VB to the CB, which induces the increasing optical absorption in the UV-light region. For Fe-doped system, there are a series of impurity states (Fe 3*d* orbital) appearing in the forbidden gap and the band gap has an obvious narrowing compared with the pure anatase TiO_2. These results indicate that the electrons are excited easily from the VB to the CB through the Fe 3*d* states under the visible-light irradiation, which can lead to a good optical absorption for Fe-doped TiO_2 in the visible-light region. For (Si,Fe)-codoped TiO_2 system, synergistic effect of (Si,Fe) codoping induces a band gap narrowing and appearing Fe 3*d* states in the forbidden gap, which lead to a decrease of

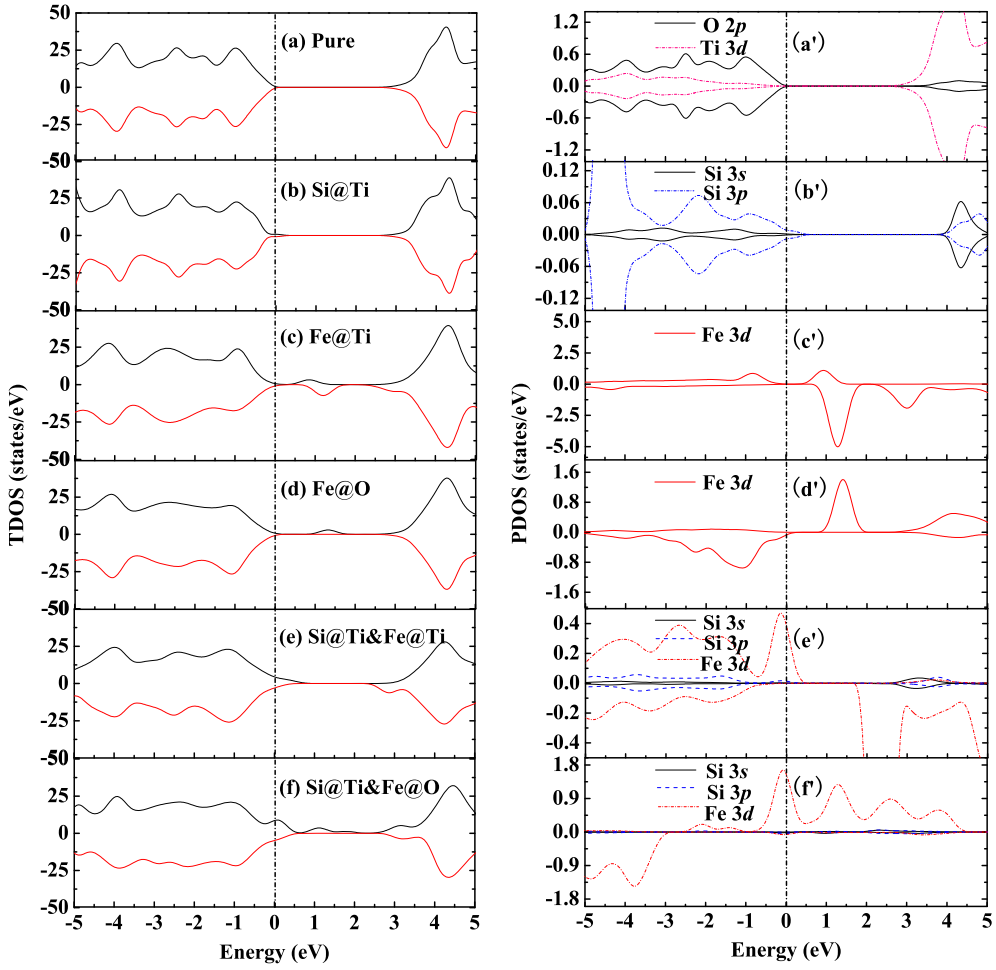

Fig. 2 – Calculated TDOS and PDOS of different doped TiO_2. The top of the valence band of pure anatase TiO_2 is taken as the reference level. Curves above and below the horizontal axis refer to the up-spin and down-spin DOS, respectively.

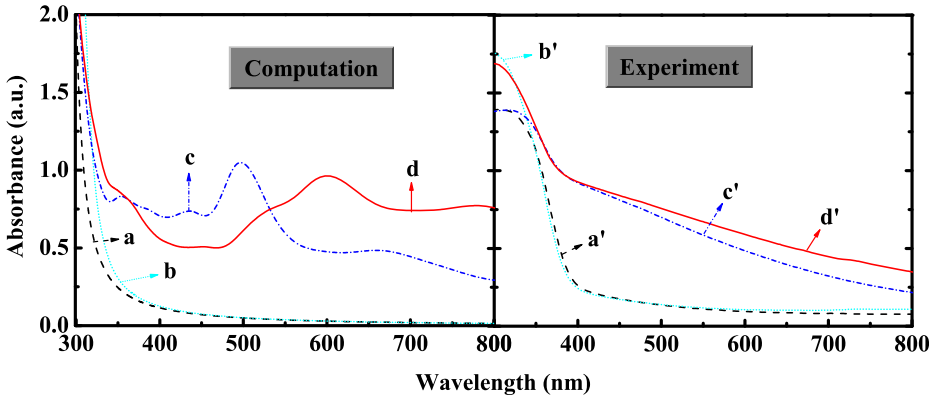

Fig. 3 – The optical absorption curves of (a, a') pure, (b, b') Si-doped, (c, c') Fe-doped, and (d, d') (Si,Fe)-codoped TiO_2. The left and right figures represent the absorption spectra obtained by computations and experiments, respectively.

the photon excitation energy in the view of electronic structure. Therefore, the absorption of visible- and UV-light is greatly enhanced in (Si,Fe)-codoped anatase TiO_2 compared with the pure, Si- and Fe-doped anatase TiO_2, which may be responsible for the redshift of optical absorption edge and the outstanding activity for hydrogen generation by photocatalytic water splitting in (Si,Fe)-codoped anatase TiO_2.

To confirm the better photocatalytic activity for hydrogen production by water splitting of the (Si,Fe)-codoped TiO_2 compared to that of pure TiO_2, we further observed the UV–vis absorption spectrum by experiments.

Nanocrystalline pure, Si-, Fe-, and (Si,Fe)-codoped TiO_2 were prepared by a sol-gel-solvothermal method. Firstly, a desired amount (0.3367 g) of $Fe(NO_3)_3{\bullet}9H_2O$ was dissolved in 39.66 mL of CH_3COOH solution under stirring. Then, 5.58 mL of $(C_2H_5O)_4Si$ was dropwise added into the solution with stirring for 1 h. Secondly, 28.36 mL of $[CH_3(CH_2)_3O]_4Ti$ was also dropwise added into the solution with continuous stirring for 2 h, and the solution was heated in an oven and kept at 140 °C for 14 h. Finally, the precipitate obtained was dried in a vacuum oven at 70 °C for 48 h. To evaluate the photocatalytic activity of samples, hydrogen generation by photocatalytic water splitting was performed in a cylindrical quartz photo-reactor with a 1000 mL capacity. A flow of dry N_2 gas was used to purge dissolved O_2 in the reactor for 30 min prior to illumination. A 500 W long-arc xenon lamp surrounded with a water cooling system was fixed in the center of the reaction cell. Photocatalyst (0.4 g) was suspended in 60 mL ethanol and 540 mL distilled water under stirring magnetically. H_2 was analyzed by gas chromatograph (GC) using a Fuli GC-9790II (ZheJiang, China), equipped with a thermal conductivity detector (TCD) and a stainless steel column (2 m) packed with molecular sieves (5 A) at 323 K.

The crystalline phase was identified by X-ray diffraction (XRD) (Rigaku D/MAX-2400). The Brunauer–Emmett–Teller (BET) surface area of the samples was measured through nitrogen adsorption at 77 K (Nova 2000e). The UV–vis absorption spectra were obtained on an UV–vis spectrophotometer (UV-3600) and using $BaSO_4$ as the reference sample.

Fig. 1(b) shows the XRD patterns of the samples of pure, Si-, Fe-, and (Si,Fe)-codoped TiO_2. It is found that all of the diffraction peaks are contributed by the anatase TiO_2 phase and no other visible impurity peak can be distinguished in the pattern of pure or doped sample. The BET surface areas for pure, Si-, Fe-, and (Si,Fe)-codoped TiO_2 are 84.21, 252.42, 226.72 and 308.31 m^2/g, respectively. It is shown that the surface area of TiO_2 powders is increased to 308.31 m^2/g with the coexistence of Si and Fe in TiO_2, about four times of that of pure TiO_2 powders.

The optical absorption spectra of the pure and doped systems are measured by experiments, and shown in Fig. 3. Compared with the pure TiO_2, it is clear that the incorporation of Si into TiO_2 lattice induces the enhanced optical absorption in the UV-light region. For Fe-doped system, it exhibits an excellent absorption activity in the visible-light region. For (Si,Fe)-codoped TiO_2, it is obvious that the optical absorption in the UV–visible region is stronger than that of pure TiO_2, especially in the visible-light region. The enhancement of absorption in the visible-light region can promote the utilization of the solar light for the doping TiO_2, which enhances the visible-light photocatalytic activity of TiO_2 for hydrogen production by water splitting. However, there are small misalignments between the experimental and theoretical results, which may be due to neglect of the anisotropy of the absorption coefficient and the well-known limitation of DFT. But, from the perspective of qualitative analysis, the experimental results are consistent with the calculations.

The photocatalytic activity of the pure and doped TiO_2 samples was evaluated by hydrogen production from water splitting, as shown in Fig. 4(a). Pure water produces very low amount of hydrogen under the visible-light irradiation without photocatalyst, indicating that the photolysis can be ignored. It is obvious that Si, Fe, and (Si,Fe) (co)doping can improve the photocatalytic activity of hydrogen production in TiO_2 material. Among them, (Si,Fe)-codoped TiO_2 sample exhibits the best photocatalytic activity of hydrogen production compared with the pure TiO_2, which may be due to a stronger absorption of solar light in (Si,Fe)-codoped TiO_2. In addition, Fig. 4(b) shows the VB and CB edge potentials of pure and (Si,Fe)-codoped TiO_2 vs. normal hydrogen electrode (NHE). The CBM potential of (Si,Fe)-codoped TiO_2 is −0.6 eV, more negative than H^+/H_2 (0 eV). The results show that it has the ability to reduce H^+ to produce H_2, and the reductive ability is stronger than pure TiO_2. Therefore, TiO_2 exhibits outstanding

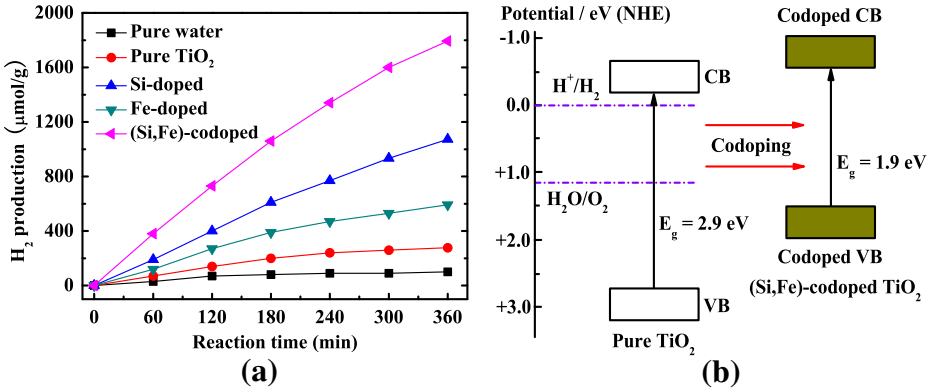

Fig. 4 – (A) Hydrogen production by water splitting as a function of reaction time over the pure and doped TiO_2 samples, and (b) a schematic diagram of band level arrangements for photocatalytic water splitting in pure and codoped TiO_2 systems.

photocatalytic activity for hydrogen production by water splitting through Si and Fe codoping.

In conclusion, we have investigated the electronic and optical properties of (Si,Fe)-codoped TiO_2 based on DFT calculations. The synergistic effects of (Si,Fe) codoping may further reduce the electrons excited energy from VB to CB compared with the pure TiO_2 under the solar light irradiation, which enhances the photocatalytic activity for hydrogen production by water splitting and induces the redshift of absorption edge. The photocatalytic splitting water and absorption spectra obtained by experiments indicate that (Si,Fe)-codoped TiO_2 sample has a much stronger absorption of the solar light and photocatalytic activity for hydrogen production by water splitting than the pure TiO_2, which verifies the reliability of the calculation results.

Acknowledgements

Yanming Lin would like to thank Dr. Kesong Yang and Dr. Run Long for helpful discussions. This work was supported by the National Natural Science Foundation of China under Grants (Nos. 10647008, 50971099, and 21176199), the Research Fund for the Doctoral Program of Higher Education (Nos. 20096101110017 and 20096101110013), Key Project of Natural Science Foundation of Shaanxi Province of China (Nos. 2010JZ002 and 2011JM1001), and Graduate's Innovation Fund of Northwest University of China (No. YZZ12082).

REFERENCES

[1] Fujishima A, Honda K. Electrochemical photolysis of water at a semiconductor electrode. Nature 1972;238:37–8.
[2] Antony RP, Mathews T, Ramesh C, Murugesan N, Dasgupta A, Dhara S, et al. Efficient photocatalytic hydrogen generation by Pt modified TiO_2nanotubes fabricated by rapid breakdown anodization. Int J Hydrogen Energy 2012;37:8268–76.
[3] Yang K, Dai Y, Huang B, Whangbo MH. Density functional characterization of the visible-light absorption in substitutional C-anion and C-cation doped TiO_2. J Phys Chem C 2009;113:2624–9.
[4] Asahi R, Morikawa T, Ohwaki T, Aoki K, Taga Y. Visible-light photocatalysis in nitrogen-doped titanium oxides. Science 2001;293:269–71.
[5] Lin YM, Jiang ZY, Zhu CY, Hu XY, Zhang XD, Fan J. Visible-light photocatalytic activity of Ni-doped TiO_2 from *ab initio* calculations. Mater Chem Phys 2012;133:746–50.
[6] Yang K, Dai Y, Huang B. Study of the nitrogen concentration influence on N-doped TiO_2 anatase from first-principles calculations. J Phys Chem C 2007;111:12086–90.
[7] Khan SUM, Al-Shahry M, Ingler Jr WB. Efficient photochemical water splitting by a chemically modified n-TiO_2. Science 2002;297:2243–5.
[8] Spadavecchia F, Cappelletti G, Ardizzone S, Ceotto M, Falciola L. Electronic structure of pure and N-doped TiO_2 nanocrystals by electrochemical experiments and first principles calculations. J Phys Chem C 2011;115:6381–91.
[9] Lu J, Dai Y, Guo M, Yu L, Lai K, Huang B. Chemicalandopticalpropertiesofcarbon-dopedTiO_2: a density–functional study. Appl Phys Lett 2012;100:102114–7.
[10] González-Borrero PP, Bernabé HS, Astrath NGC, Bento AC, Baesso ML, Castro Meira MV, et al. Energy-level and optical properties of nitrogen doped TiO_2: an experimental and theoretical study. Appl Phys Lett 2011;99:221909–11.
[11] Zhao D, Huang X, Tian B, Zhou S, Li Y, Du Z. The effect of electronegative difference on the electronic structure and visible light photocatalytic activity of N-doped anatase TiO_2 by first-principles calculations. Appl Phys Lett 2011;98:162107–9.
[12] Xing MY, Li WK, Wu YM, Zhang JL, Gong XQ. Formation of new structures and their synergistic effects in boron and nitrogen codoped TiO_2 for enhancement of photocatalytic performance. J Phys Chem C 2011;115:7858–65.
[13] Jia L, Wu C, Li Y, Han S, Li Z, Chi B, et al. Enhanced visible-light photocatalytic activity of anatase TiO_2 through N and S codoping. Appl Phys Lett 2011;98:211903–5.
[14] Long R, English NJ. Synergistic effects on band gap-narrowing in titania by codoping from first-principles calculations. Chem Mater 2010;22:1616–23.
[15] Lin Y, Jiang Z, Hu X, Zhang X, Fan J. The electronic and optical properties of Eu/Si-codopedanatase TiO_2 photocatalyst. Appl Phys Lett 2012;100:102105–8.
[16] Li N, Yao KL, Li L, Sun ZY, Gao GY, Zhu L. Effect of carbon/hydrogen species incorporation on electronic structure of anatase-TiO_2. J Appl Phys 2011;110:073513–7.
[17] Su Y, Xiao Y, Li Y, Du Y, Zhang Y. Preparation, photocatalytic performance and electronic structures of visible-light-driven Fe–N-codopedTiO_2 nanoparticles. Mater Chem Phys 2011;126:761–8.

[18] Long R, English NJ. Band gap engineering of (N, Si)-codoped TiO_2 from hybrid density functional theory calculations. New J Phys 2012;14:053007–17.
[19] Gai Y, Li J, Li SS, Xia JB, Wei SH. Design of narrow-gap TiO_2: a passivated codoping approach for enhanced photoelectrochemical activity. Phys Rev Lett 2009;102:036402–5.
[20] Lin Y, Jiang Z, Zhu C, Hu X, Zhang X, Zhu H, et al. Enhanced optical absorption and photocatalytic activity of anatase TiO_2 through (Si, Ni) codoping. Appl Phys Lett 2012;101:062106–10.
[21] Kresse G, Hafner J. *Ab initio* molecular-dynamics simulation of the liquid-metal–amorphous-semiconductor transition in germanium. Phys Rev B 1994;49:14251–69.
[22] Kresse G, Furthmüller J. Efficient iterative schemes for *ab initio* total-energy calculations using a plane-wave basis set. Phys Rev B 1996;54:11169–86.
[23] Perdew JP, Ahevary CJ, Vosko SH, Jackson KA, Pederson MR, Singh DJ, et al. Atoms, molecules, solids, and surfaces: applications of the generalized gradient approximation for exchange and correlation. Phys Rev B 2004;46:6671–87.
[24] Monkhorst HJ, Pack JD. Special points for Brillouin-zone integrations. Phys Rev B 1976;13:5188–92.
[25] Dudarev SL, Botton GA, Savarsov SY, Humphreys CJ, Sutton AP. Electron-energy-loss spectra and the structural stability of nickel oxide: an LSDA+U study. Phys Rev B 1998;57:1505–9.
[26] Tang H, Lévy F, Berger H, Schmid PE. Urbach tail of anatase TiO_2. Phys Rev B 1995;52:7771–4.
[27] Yang K, Dai Y, Huang B. First-principles calculations for geometrical structures and electronic properties of Si-doped TiO_2. Chem Phys Lett 2008;456:71–5.